JOURNAL OF SOLID STATE CHEMISTRY **133,** 264–268 (1997)
ARTICLE NO. SC977453

FT Raman Spectroscopy of Some Metal Hexaborides

R. Schmechel and H. Werheit

Solid State Physics Laboratory, Gerhard Mercator University Duisburg, D 47048 Duisburg, Germany

and

Yu. B. Paderno

I.N. Frantsevich Institute for Problems of Materials Science, Ukrainian Academy of Sciences, 252142 Kiev, Ukraine

Received April 14, 1997; accepted April 28, 1997

Fourier-transform Raman (FT) spectra of single-crystal LaB_6 and SmB_6 and of sintered $EuB_{6-X}C_X$ ($X \approx 0.1$) were measured at room temperature. For excitation a Nd:YAG laser with about 2 W irradiation power was used. The spectra exhibited many more details of the phonon densities of states than those obtained with conventional Raman spectroscopy by other authors. In particular two low-energy peaks were found at 104 and 204 cm^{-1}, which can be easily attributed to the acoustical and the lowest optical branches. The FT Raman spectra of LaB_6 agree well with the phonon densities of states determined by other experimental methods and theoretical calculation, while for SmB_6 a considerable softening of the optical modes is observed, which is probably due to nonlinear effects in consequence of the high excitation power used in the FT Raman spectrometer.

INTRODUCTION

Octahedral B_6 clusters and single transition elements form the CsCl-type crystal structure of the metal hexaborides. Their representatives are mostly metals and sometimes semiconductors. They exhibit interesting physical phenomena like intermediate valency, superconductivity, dense Kondo systems, and anomalous magnetism. Some MB_6 compounds belong to the best thermionic materials. For reviews see, e.g., (1, 2) and references therein.

To determine the relation between electronic properties and lattice dynamics a detailed knowledge of the phonon spectra is necessary. Ishii *et al.* (3) determined the A_{1g}, E_g, and F_{2g} vibration modes of the B_6 octahedron of EuB_6 and GdB_6 by Raman scattering; Mörke *et al.* (4) found additional single lines in the Raman spectra at 214 cm^{-1} for LaB_6 and at 172 cm^{-1} for SmB_6. Crystal defects are assumed to break the selection rules for Raman scattering in these cases. Phonon dispersion curves and phonon densities of states were calculated by Schell *et al.* (5, 6) and compared with phonon densities determined by inelastic neutron scattering. Point contact spectroscopy yielded the whole phonon spectrum of single crystal LaB_6 (7). The dispersion curves of acoustical and optical phonons were determined for $La^{11}B_6$ and $^{154}Sm^{11}B_6$ by inelastic neutron scattering (8, 9)

Using the same experimental method Smith *et al.* (10) determined the dispersion curves of acoustic and optical phonons of $La^{11}B_6$, and they measured the specific heat of LaB_6 and YbB_6 as a function of temperature. An improved density of states calculation was reported by Gompf *et al.* (11) Schneider *et al.* (12) determined the phonon density of states from electron tuneling experiments into superconducting YB_6.

In this paper we present Fourier-transform (FT) Raman spectra of LaB_6, SmB_6, and $EuB_{6-X}C_X$ ($X \approx 0.1$), which show many more details of the phonon densities of states than the previous Raman measurements, in particular in the case of LaB_6.

SAMPLE MATERIAL

The LaB_6 and SmB_6 single crystals were grown by the induction zone melting method. The source borides used were obtained by the reduction of high-purity oxides of the correspondent metals with amorphous boron. According to the chemical analysis the composition of the zone-melted LaB_6 is slightly shifted to the boron deficite side; SmB_6 is close to the ideal stochiometric composition. The existence of defects in the metal and boron sublattices cannot be excluded.

The $EuB_{6-X}C_X$ ($X \approx 0.1$) samples (ESK Kempten) were prepared by sintering (13) leading to pellets of nearly theoretical density. The carbon atoms are assumed to substitute for boron in the octahedra thus diluting the lattice.

0022-4596/97 $25.00

Accordingly the carbon content was derived from the lattice constants determined by X-ray diffraction (14).

EXPERIMENTAL

For the measurements a commercial FT Raman supplement equipment of the FTIR spectrometer 113v (Bruker, Karlsruhe) was used. It contains a Nd:YAG laser (1.07 μm = 1.16 eV)) as the excitation source. This laser allows powers up to 4 W. The measurements were performed largely in back scattering geometry with an incident power of about 2.5 W/mm^2 of the laser at the sample. The rise in temperature caused by this excitation was negligible in the case of LaB_6 and SmB_6 and about 50 K in the case of $EuB_{5.9}C_{0.1}$ probably because of porosity.

RESULTS

Figures 1a–1c show the FT Raman spectra of LaB_6, SmB_6, and $EuB_{6-X}C_X$ ($X \approx 0.1$); the spectral resolution is 2 cm^{-1}. To reduce the noise of the interferograms large numbers of interferometer scans were averaged, before the Fourier transformation was performed (2000 for LaB_6, 10,000 for SmB_6, and 1000 and 7000 respectively for $EuB_{5.9}C_{0.1}$). For LaB_6 the comparison of the Stokes and anti-Stokes ranges of the FT Raman spectrum confirms the fine structure of the Raman band at 110 cm^{-1}.

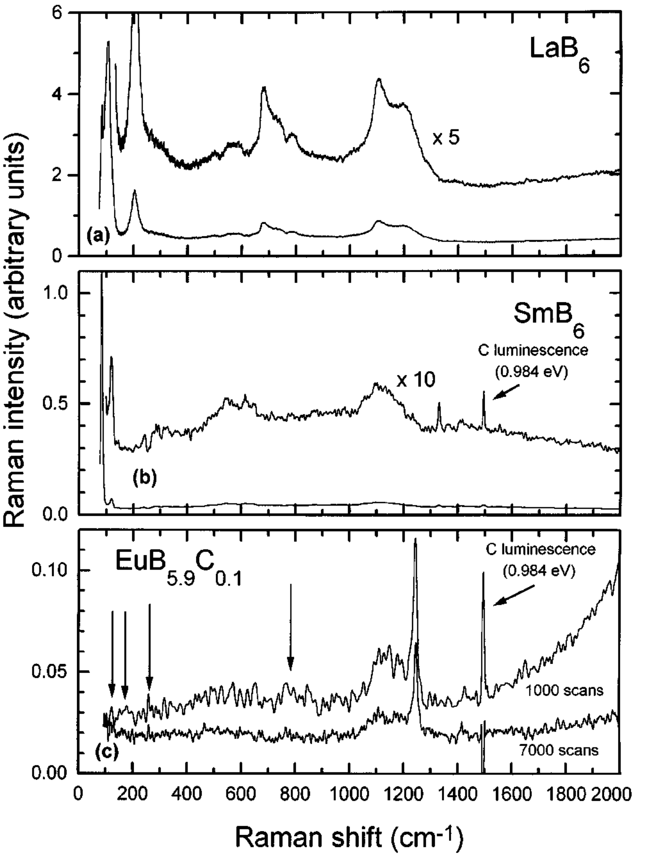

FIG. 1. FT Raman spectra of (a) LaB_6, (b) SmB_6, and (c) $EuB_{5.9}$ $C_{0.1}$. The attribution of the peaks at 0.984 eV in SmB_6, and $EuB_{5.9}$ $C_{0.1}$ to carbon luminescence is provisional only (see text).

Compared with the results of Mörke *et al.* (4) our spectra obtained on LaB_6 and SmB_6 show distinctly broader A_{1g}, E_g, and F_{2g} bands though the resolution of our spectra is four times higher than theirs (2 and 8 cm^{-1} respectively). Accordingly this broadening must be attributed to physical reasons within the materials investigated. These physical reasons could have their origin either in the quality of crystals or in the method of measurement, which could lead to non-linear effects because of the high excitation intensity. The clarification of this question requires further investigations. Otherwise some more detailed structures of the already known bands and some additional weak bands can be seen in our FT Raman spectra. In particular our spectra of LaB_6 and SmB_6 exhibit two strong structured Raman bands in the range of the acoustical and low-frequency optical phonons, while in the spectra of Mörke et al there is only one weak band, each. However, in the Raman spectrum of $EuB_{5.9}C_{0.1}$ the position of the acoustical phonons can be at best guessed from some weak but obviously reproducible structures in that range.

DISCUSSION

For LaB_6 the FT Raman spectra can be compared with results on the phonon densities obtained by other methods. Figure 2 shows the comparison with the phonon branches determined by inelastic neutron scattering on $La^{11}B_6$ by Smith *et al.* (10). This allows the attribution of the 104 cm^{-1} Raman band to the acoustical phonon branch at the boundary of the Brillouin zone and of the 204 cm^{-1} band to the lowest optical phonon branches at the Γ point. At least some of the weaker density of states maxima of these branches at the boundary of the Brillouin zone are discernible in the FT Raman spectrum.

In Fig. 3 the FT Raman spectra are compared with the density of states derived experimentally from inelastic neutron scattering by Schell *et al.* (6), determined by point contact spectroscopy by Samuely et al. (7) and theoretically calculated by Schell *et al.* (6) and Gompf *et al.* (5). In particular at low energies the agreement is quite good in all cases. According to the authors the neutron scattering experiments failed at higher energies. The two theoretical calculations fit the different phonon bands differently well. The agreement with the point contact spectrum is quite good; only the double peak at about 1100/1200 cm^{-1} is shifted.

Mörke *et al.* (4) assume that the selection rules forbidding Raman scattering of phonon modes apart form those, which

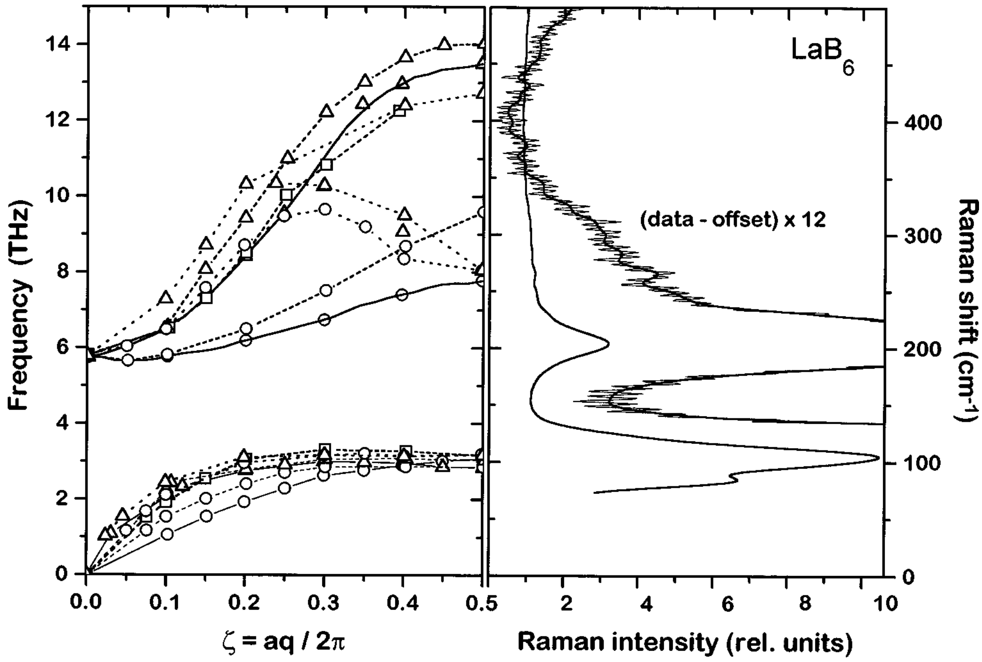

FIG. 2. Low frequency part of the FT Raman spectrum of LaB_6 compared with the phonon branches obtained on $La^{11}B_6$ by inelastic neutron scattering reproduced from Smith *et al.* (10) (the results for all crystallographic directions are collected in the diagram).

are Raman active for symmetry reasons, are lifted in their samples because of crystal defects. Obviously in our spectra of LaB_6 and SmB_6 the selection rules are considerably more lifted. We attribute this to the very strong optical excitation density. Probably similarly to the icosahedral boron-rich solids, the boron cages are distorted because of an electron–phonon interaction of optically excited carriers. However, it is surprizing that in the FT Raman spectra of

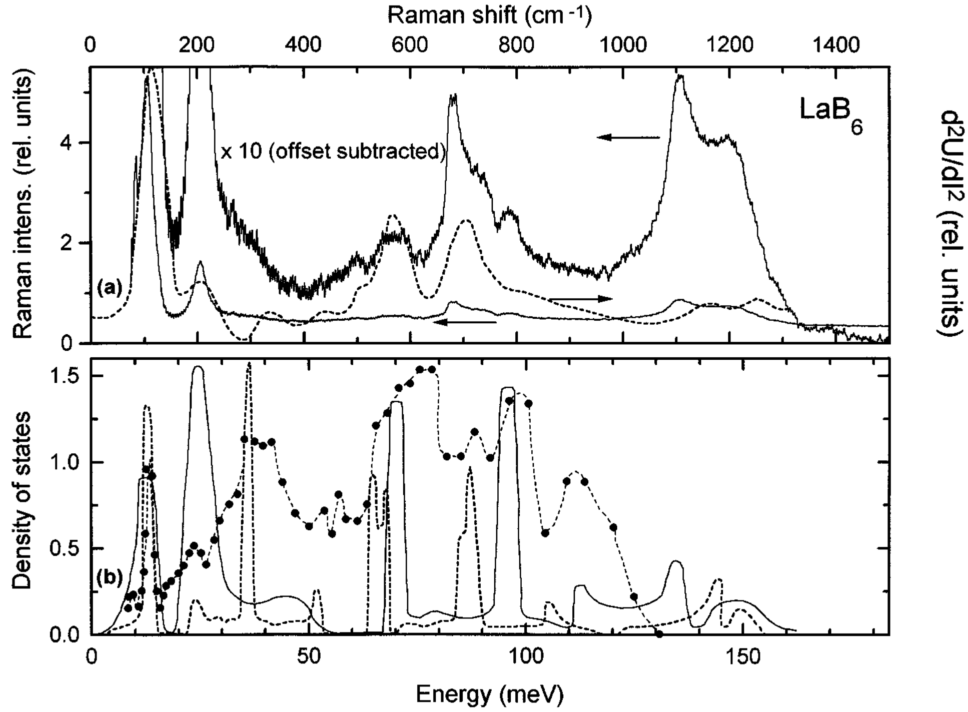

FIG. 3. Entire phonon spectrum of LaB_6. (a) FT Raman spectrum compared with point contact spectrum reproduced from Samuely *et al.* (7). (b) Solid circles, density of states determined by inelastic neutron scattering (reproduced from Schell *et al.* (6)); solid line, theoretically calculated density of states by Schell *et al.* (6); and broken line, theoretically calculated by Gompf *et al.* (5).

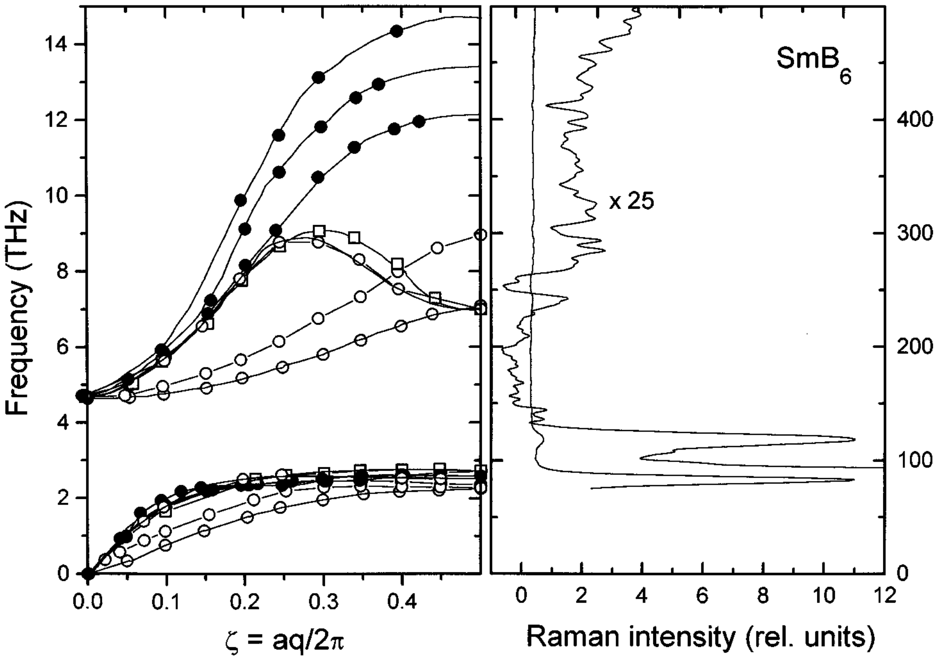

FIG. 4. Low frequency part of the FT Raman spectrum of SmB_6 compared with the phonon branches obtained on $^{154}Sm^{11}B_6$ by inelastic neutron scattering reproduced from Alekseev *et al.* (8, 9) (the results for all crystallographic directions are collected in the diagram).

$EuB_{5.9}C_{0.1}$, despite the crystal defects doubtlessly introduced by the carbon atoms substituting for boron in the octahedra, the acoustical phonons can be guessed at best.

For SmB_6 there is a considerable difference between the phonon resonance frequencies obtained from the FT Raman spectrum and the phonon dispersion curves obtained by inelastic neutron scattering on $^{154}Sm^{11}B_6$ by Alekseev *et al.* (8, 9) (see Fig. 4). While the acoustical phonon branch is exactly confirmed, the next maximum in the FT Raman spectrum, which is obviously to be attributed

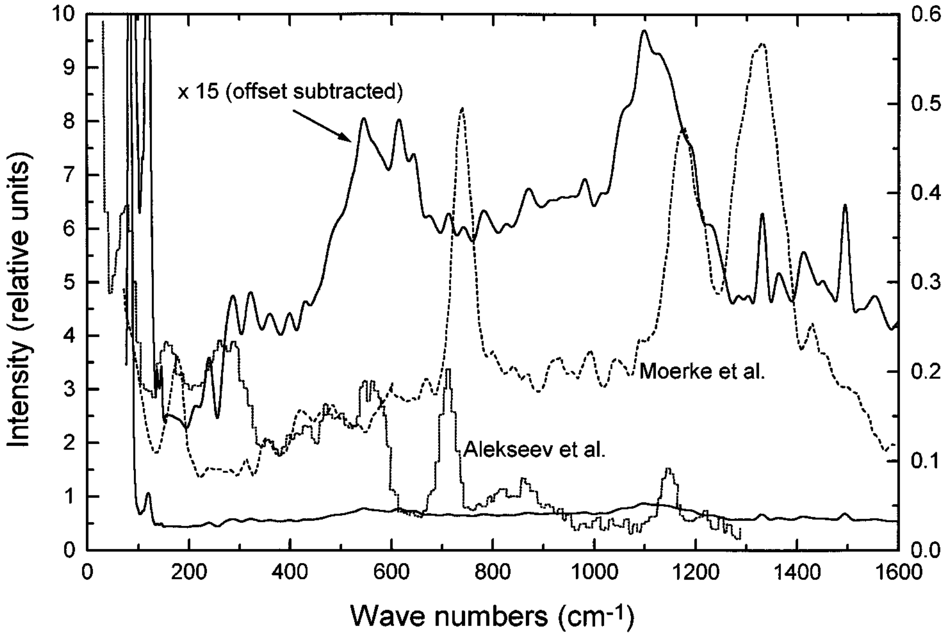

FIG. 5. Entire phonon spectrum of SmB_6. Full lines, FT Raman spectrum (present work); broken line, conventionally measured Raman spectrum, reproduced from Moerke *et al.* (4); and dotted line, inelastic neutron scattering, reproduced from Alekseev *et al.* (9).

to the lowest optical phonon branch, is distinctly shifted toward lower frequencies compared with the density of states maximum at $\zeta = 0$ of the neutron scattering results. This is confirmed for the phonons at higher frequencies as well: Compared with the Raman spectrum obtained by Moerke *et al.* (5) all the FT Raman peaks are considerably shifted toward lower frequencies (see Fig. 5) In this spectral range Alekseev's results obtained by inelastic neutron scattering seems to exhibit peaks at intermediate positions between both Raman results. It seems that in intermediate valent SmB_6 the well-known phonon softening depends considerably on the actual condition of measurement. In particular the high excitation intensity in the FT Raman equipment enhances this phonon softening in SmB_6 considerably.

In the spectra of SmB_6 and $EuB_{5.9}C_{0.1}$ there are distinct narrow peaks at 0.984 eV, while there is no such peak in the spectrum of LaB_6. We attribute this peak provisionally to the luminescence of carbon, because its intensity roughly agrees with the carbon content in $EuB_{5.9}C_{0.1}$ being distinctly higher than in SmB_6, and because a strong luminescence line due to a carbon complex in silicon at almost the same energy (0.969 eV) is known (see (15)). Of course, the final attribution requires further systematic investigations.

ACKNOWLEDGMENT

The authors are grateful to Dr. K. A. Schwetz, ESK Kempten, for providing the $EuB_{6-X}C_X$ samples.

REFERENCES

1. M. Kasaya and F. Iga, *in* "Boron-Rich Solids," (D. Emin, T. Aselage, C. L. Beckel, I. A. Howard, and C. Wood, Eds.), AIP Conf. Proc. 140, p. 11. Albuquerque, NM, 1985.
2. P. Wachter, *in* "Proc. 9th Int. Symp. Boron, Borides and Related Comp. Duisburg, University of Duisburg, 1987" (H. Werheit, Ed.), p. 166.
3. M. Ishii, M. Aono, S. Muranaka, and S. Kawai, *Solid State Comm.* **20,** 437 (1976).
4. I. Mörke, V. Dvorak, and P. Wachter, *Solid State Comm.* **40,** 331 (1981).
5. F. Gompf, *in* "Progress Report Teilinstitut Nukleare Festkörperphysik" (K. Käfer, Ed.), p. 17. Kernforschungszentrum Karlsruhe KfK 2670, 1978.
6. G. Schell, H. Winter, H. Rietschel, and F. Gompf, *Phys. Rev. B* **25,** 1589 (1982).
7. P. Samuely, M. Reiffers, K. Flachbart, A. I. Akimenko, J. K. Janson, N. M. Ponomarenko, and Yu. B. Paderno, *J. Low Temp. Phys.* **71,** 49 (1988).
8. P. A. Alekseev, A. S. Ivanov, K. A. Kikoin, A. S. Mischenko, A. N. Lasukov, A. Yu. Rumyantsev, I. P. Sadikov, E. S. Konovalova, Yu. B. Paderno, B. Dorner, and H. Shober, *in* "Lattice Dynamics in Fluctuating Valence Compound SmB," (D. Emin, T. L. Aselage, A. C. Switendick, B. Morosin, and C. L. Beckel, Eds.), AIP Conf. Proc. 231, p. 318. Albuquerque, NM, 1991.
9. P. A. Alekseev, A. N. Lasukov, K. Osborn, B. Rainford, I. P. Sadikov, E. S. Konovalova, and Yu. B. Paderno, *Europhys. Lett.* **23,** 347 (1993).
10. H. G. Smith, G. Dolling, S. Kunii, M. Kasaya, B. Liu, K. Takegahara, T. Kasuya, and T. Goto, *Solid State Comm.* **53,** 15 (1985).
11. F. Gompf, G. Schell, and H. Winter, *in* "Progress Report, Teilinstitut Nukleare Festkörperphysik des Instituts für Angewandte Kernphysik" (K.-P. Bohnen and M. Kobbelt, Eds.), p. 20. Kernforschungszentrum Karlsruhe KfK 2881, 1979.
12. R. Schneider, J. Geerk, and H. Rietschel, *Europhys. Lett.* **4,** 845 (1987).
13 H. Knoch, K. A. Schwetz, E. Bechler and A. Lipp, "Proc. 9th Int. Symp. Boron, Borides and Related Comp. Duisburg, University of Duisburg, 1987" (H. Werheit, Ed.), p. 442.
14. K. A. Schwetz, personal communication, 1996.
15. G. Davies, *Phys. Rep.* **176,** 84 (1989).